

SMECTITE-ILLITE-MUSCOVITE TRANSFORMATIONS, QUARTZ DISSOLUTION, AND SILICA RELEASE IN SHALES

PETER C. VAN DE KAMP*

40385 Queener Drive, Scio, Oregon 97374, USA

Abstract—Quantitative analysis of the smectite-to-illite and illite-to-muscovite transformations indicates that 17–28 wt.% SiO₂ and 17–23 wt.% SiO₂, respectively, are liberated during these reactions, assuming that Al is conserved. Dissolution of quartz silt in shales yields up to 6–9% SiO₂ in the range up to 200°C and a further 10–15% SiO₂ in the 200–500°C range. For muds altered to shales at 200°C, 14–20 wt.% silica is evolved. From 200 to 500°C, a further 18–28 wt.% silica is evolved. Additional small amounts of silica may be released in the alteration of feldspar to clay and by stylolitization of quartz silt. Thus, in the burial and temperature range of diagenesis into the epizone, major quantities of silica are released from clays and by quartz dissolution in shales. Within this range of alteration, concomitant decline of whole-rock Si/Al (SiO₂/Al₂O₃) in the transformation of smectite to illite to muscovite suggests the liberated silica migrates from the source shale. As a result, the metamorphosed shales are more micaceous and less quartzose than their progenitor muds. In the diagenetic zone and anchizone, the evolved silica is probably a major source of quartz cement in sandstones. In the epizone, evolved silica is commonly present in quartz veins in the parent rocks. Fluid-inclusion temperatures in quartz overgrowths and fracture fillings in some sandstones suggest that some cements may have been derived from downdip basinal shales and pressure solution in sandstones.

Key Words—Anchizone, Clay Transformation, Diagenesis, Epizone, Illite, Muscovite, Quartz, Silica, Smectite.

INTRODUCTION

The purpose of this study was to quantitatively evaluate the chemistry of the transformation of smectite to mixed-layer illite-smectite and illite, and then to muscovite, with the goal of estimating the amount of silica released. Alumina was assumed to be conserved, as indicated by Wintsch and Kvale (1994) and Land *et al.* (1997). Dissolution of quartz and feldspar silt as sources of silica during burial alteration of shale was also evaluated. The fate of the released silica was considered; is it largely expelled from the shale hosts or is much of it retained as silica minerals in the shales? Is the free silica a significant source of cement in sandstones? What is the evidence for silica migration from shales to sandstones? This evaluation is related to temperatures and burial depths in the range of diagenesis to amphibolite-facies metamorphism. Existing mineral and chemical data for clays and shales were evaluated and significant new data are presented for shales altered in the range 100–500°C.

The smectite (montmorillonite)-to-illite transformation in shales as a source of silica for sandstone cement was studied by Towe (1962), Leder and Park (1986), Boles and Franks (1979), Lynch (1997), and Land and Milliken (2000). It is well understood that relatively siliceous smectite clays alter to less siliceous illite with increasing depth of burial and temperature in sedimentary basins (Hower *et al.*, 1976; Lynch *et al.*, 1997). On the basis of

whole-rock analyses of shales buried at depths of 2.4 to 5.5 km, Land *et al.* (1997) estimated a loss of ~6 wt.% SiO₂. In the mixed-layer smectite-illite series, with continuing deeper burial and greater temperatures, the proportion of smectite decreases as the illite content increases. Ultimately, from illite, the thermodynamically stable muscovite is developed. Accompanying the mineralogical alterations are chemical changes including loss of silica and water and uptake of K. Reactions which may accompany the smectite transformation are alteration of K-feldspar and plagioclase to clays, silica, and/or albite (Lynch *et al.*, 1997). The transformation of smectite to ~95% illite occurs in the temperature range 20–200°C, and the 95% illite-to-muscovite transformation in the 200–300°C range (Merriman and Frey, 1999). With increasing temperature from ~300 to 500°C, very fine crystalline muscovite is gradually replaced by thermodynamically stable, coarse muscovite (Merriman and Peacor, 1999). These alterations and their relations to diagenetic and metamorphic zones are summarized in Figure 1a. Important to note is that through the range of diagenesis and into the epizone of metamorphism, a regular progression is observed from silica-rich smectite to relatively silica-poor muscovite.

In sedimentary basins, there has been extensive quantitative analysis of authigenic quartz cement volumes in sandstones buried deeper than ~3 km at temperatures of 90–100°C+ (Stone and Siever, 1996; Giles *et al.*, 2000). Potential sources of quartz cement in sandstones include: (1) internal, *i.e.* pressure solution of detrital quartz (Thomson, 1959; Thomas *et al.*, 1993; Spötl *et al.*, 2000; Hartmann *et al.*, 2000; Walderhaug and Bjorkum,

* E-mail address of corresponding author:
pvdkfarm@wvi.com
DOI: 10.1346/CCMN.2008.0560106

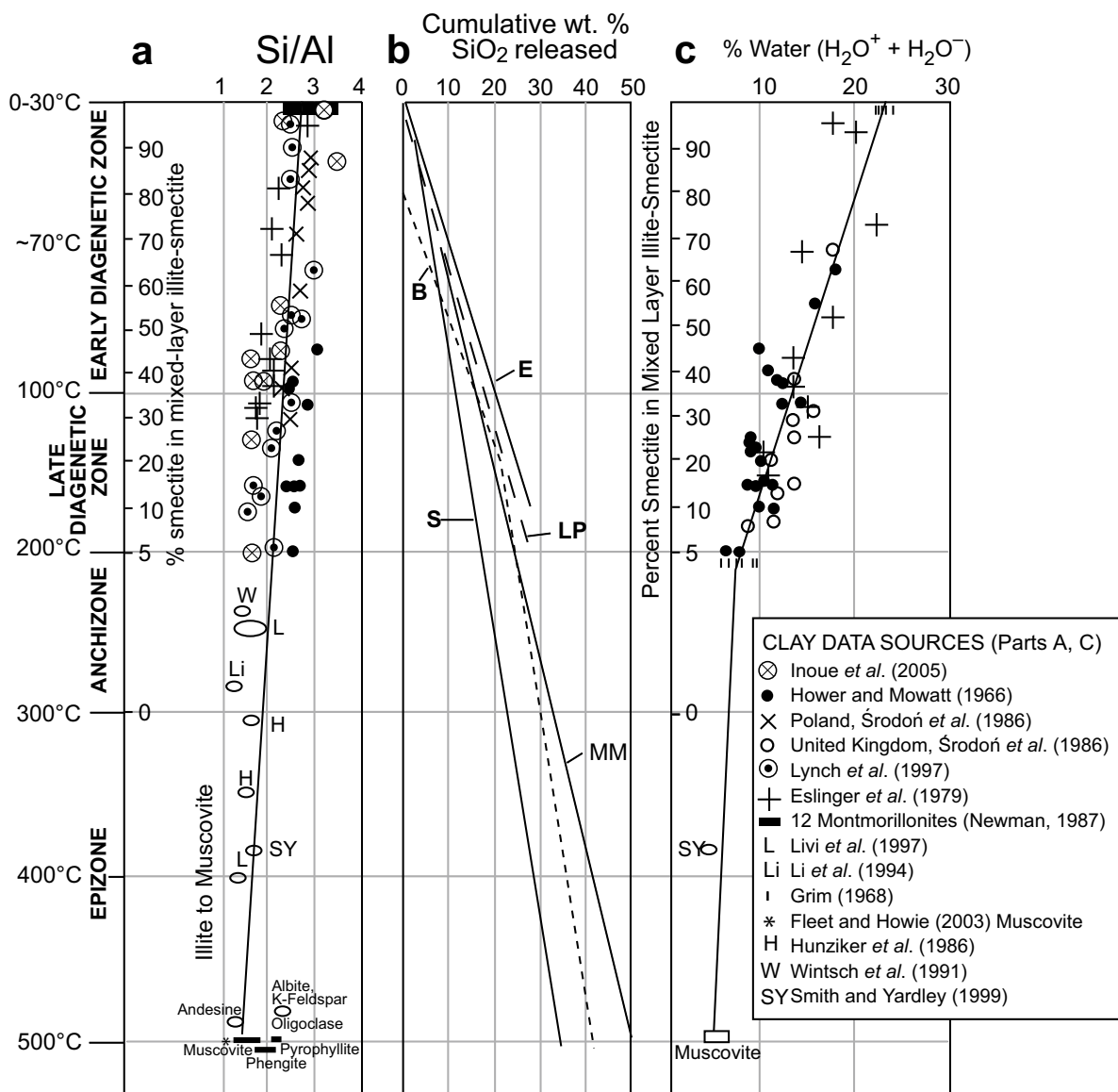


Figure 1. (a) Plot of Si/Al vs. temperature for the smectite–illite series, muscovite, and feldspars. Essentially, there is a regular decline of Si/Al from smectite to muscovite through the mixed-layer illite–smectite transition. For the smectite–illite series, scatter along the linear trend may be due to some clays being more aluminous than others of similar gross composition. Scatter may also be due to the presence of quartz impurity in the clay analyzed. The temperatures and diagenetic and metamorphic zones are from Merriman and Frey (1999). (b) The evolution of silica with increasing temperature, calculated in wt.%, from the smectite–muscovite series. Published estimates plus those from this study are shown. Line B indicates the 20% illite/80% smectite of Boles and Franks (1979) altered to illite and muscovite; see text for calculated estimates. Line E is for smectite to illite from Eslinger *et al.* (1979). LP is the smectite to illite alteration as indicated by Leder and Park (1987). Line S indicates estimated silica released from montmorillonite altered to 94% illite from Środoń *et al.* (1986) and thence to muscovite. MM represents estimated silica evolved in the smectite to muscovite transformation. (c) Total water content (H_2O^- plus H_2O^+) plotted for smectite–illite and muscovite illustrating the decrease in water over the range from smectite to illite and muscovite. Note that in the range of ~30°C to 200°C, ~70% of the water originally contained in smectite is lost.

2003) as well as silica freed in the alteration of detrital feldspars (Gold, 1987; Wilkinson *et al.*, 2001); and (2) external, silica transported in solution into sandstones (Burley *et al.*, 1989; Gluyas and Coleman, 1992; Gluyas *et al.*, 2000). In some cases, pressure solution (stylolitization) provides much if not all of the quartz cement in

sandstones (Walderhaug, 1994; Walderhaug and Bjorkum, 2003). Consideration of potential sources of silica for cement indicates that, in many cases, volumetrically insufficient free silica is generated within the sandstones to provide all of the 15–30% cement found in these rocks (Stone and Siever, 1996). Giles *et al.* (2000) summarized

quantitative modal data on quartz-rich sandstones from four basins to indicate: (1) an initial phase of up to 7–8% quartz cement, deposited at <90°C; and (2) a second phase of quartz cementation, ranging up to 30% by volume occurs at 90°C and above. Similar data have been cited by Stone and Siever (1996). Fluid inclusion temperatures indicate that volumetrically significant (>5%) precipitation of quartz cements commences at 70–100°C in Mesozoic sandstones of the North Sea (Bjorlykke and Egeberg, 1993; Walderhaug, 1994; Marchand *et al.*, 2002) and in the Ordovician Simpson Group of Oklahoma (Mitcheltree, 1997). Much of the observed quartz cement apparently migrated into the sandstones from a source or sources outside the sandstones. If so, what was the source of the quartz cement? Within the sequence of sandstones and associated shales, is it possible to develop and migrate the volume of cement observed in the sandstones?

MATERIALS AND METHODS

Data sources include published chemical and X-ray diffraction (XRD) analyses of clays, micas, and shales, plus new mineral and chemical analyses of muds and shales from several basins (Tables 1 and 2). The new data include 28 Ordovician Simpson Group shales associated with orthoquartzites in the Anadarko Basin of Oklahoma. These samples, from petroleum well cores, represent alterations to 6 km depth and temperatures up to 150°C. Additional new data were collected for six Lower Tertiary and Upper Cretaceous feldspathic shales interbedded with feldspathic sandstones in the Santa Ynez Mountains of California, 12 Silurian and Ordovician shales interbedded with quartzites in the Variscan Belt of northwestern Spain, and five Archean shales interbedded with quartz-rich sandstones at Sandy Lake, northwest Ontario. For comparison with the ancient rocks, modern muds were used. The mean of 58 Amazon Fan muds (Shipboard Scientific Party, 1995) represents detritus from provenance of basement and sedimentary rocks developed in temperate to intense tropical weathering. The mean of 50 Gulf of Mexico (GOM) muds from the Mississippi Fan (Pickering and Stow, 1986) is for detritus derived from basement and sedimentary provenance under temperate climate conditions. The mean for 40 non-marine California muds (present author's data) represents sediments largely derived from the plutonic and metamorphic rocks of the Sierra Nevada and southern California basement provenance in temperate climate.

New XRD analyses for this study were by K/T GeoServices, Argyle, Texas. The analytical procedures are described below. First, rock samples were reduced to fine sand size using a mortar and pestle. A split of each sample was transferred to de-ionized water and pulverized in a McCrone micronizing mill. The resulting powder was then dried, disaggregated, and pressure-packed into an aluminum sample holder to produce random-oriented whole-rock mounts. A separate sample

split was dispersed in dilute sodium phosphate solution using a sonic probe. The suspension was then size-fractionated by means of a centrifuge in order to isolate the <4 µm (equivalent spherical diameter) fraction. The suspensions were then vacuum deposited on nylon membrane filters to produce oriented clay mineral aggregates. Membrane mounts were attached to glass slides and exposed to ethylene glycol vapor for a minimum of 24 h.

X-ray diffraction analyses of the samples were performed using a Rigaku automated powder diffractometer equipped with a Cu X-ray source (40 kV, 35 mA) and a scintillation X-ray detector. The whole-rock samples were analyzed over an angular range of 2–65°2θ at a scan rate of 1%/min using a sample spinner to reduce the effects of preferred orientation. The glycol-solvated, oriented clay mounts were analyzed over an angular range of 2–50°2θ at a scan rate of 1.5%/min.

Semi-quantitative determinations of whole-rock mineral mounts were performed by utilizing integrated peak areas (derived from peak-decomposition/profile-fitting methods) and empirical reference intensity ratio (RIR) factors determined specifically for the diffractometer used in data collection. The total phyllosilicate (clay + mica) abundance of the samples was determined from the whole-rock XRD patterns using combined 001 and *hkl* clay mineral reflections and suitable empirical RIR factors.

The XRD patterns from glycol-solvated, clay-fraction samples were analyzed using techniques similar to those described above. The relative amounts of phyllosilicate minerals were determined from the patterns using profile-fitted integrated peak intensities and combined empirical and calculated RIR factors. Determinations of mixed-layer clay, ordering, and expandability were carried out by comparing experimental diffraction data from the glycol-solvated clay aggregates with simulated, one-dimensional diffraction profiles generated using the NEWMOD program written by R.C. Reynolds.

Thin sections of shales and siltstones were examined for mineralogy, insofar as it could be determined, and textures. Anchizone and epizone rocks, being coarser-grained, are amenable to thin-section analysis. Many of the shales studied are dominated by laminated clay-rich beds; some rocks contain 1–5 mm thick silt layers comprising quartz, feldspar, heavy minerals, detrital micas, and clays.

The chemical analyses of rocks were performed by Activation Laboratories, Ancaster, Ontario, Canada. The rock samples were crushed to 50–100 mesh in a mild-steel jaw crusher. The resultant sand-size material was then reduced to <200 mesh size in an agate mortar. Splits of the rock powder were mixed with a flux of lithium metaborate and lithium tetraborate, and fused in an induction furnace. The melt was immediately poured into a 5% nitric acid solution containing an internal standard and mixed continuously for ~30 min until

Table 1. Mean mineral compositions (wt.%) of shales and muds.

Site/formation	Lithology	Metamorphic grade	#Samples analyzed	Quartz range	K-feldspar	Plagioclase	Carbonate	Kaolinite	Smectite and mixed-layer illite-smectite	Chlorite	Muscovite	Pyrophyllite
Gulf of Mexico (GOM) ¹	Mud	Pleistocene-modern	37	7	3–11	2% unspecified feldspar	7	17	40	11	16	
California ²	Mud, silt	Pleistocene-modern	15	20	9–35	3	20	4	27	21	5	X
Amazon Fan ³	Mud	Pleistocene-modern	58	X	X	X	X	X	X	X	X	
Simpson Group*	Shale	Diagenetic zone	18	13	9–29	9	11					
Cozy Dell/Matilija*	Shale	Late diagenetic zone	6	17	15–23	2	15	1				
Juncal Fm.*	Shale	Late diagenetic zone	7	19	10–26	3	19	2				
Jalama Fm.*	Shale	Late diagenetic zone	5	26	12–38	3	36	1				
Llandover Shales ⁴	Shale	Anchizone	6	X	X							
Martinsburg Fm. ⁵	Shale	Anchizone	17	X	X							
Applecross Fm. ⁹	Shale	Anchizone	7	36	16–50	13	16	1				
Formosa Fm. ⁶	Shale	Anchizone	12	13	6–24	7% unspecified feldspar						
Luarca Fm. ⁶	Shale	Epizone	12	17	4–31							
Keewaywin Fm.*	Shale, siltstone	Epizone	10	15	<5–23	13	3					
Burgess Shale ⁷	Shale	Epizone	4	X								
Kidd Creek	Shale	Epizone	11	X								
DDH-A ⁸												

* New data developed for this study

¹ Data from Pickering and Stow (1986), Table 1. Hole 616, core sections 2–6 to 10–1 and 33 to 34–1 (5 samples); Hole 620, core sections 13–2 to 44–3 (32 samples).² New data by author. Samples include muds and silty muds from streams and cores of lacustrine deposits.³ Data from Shipboard Scientific Party (1995), Holes 931–937, 940–942⁴ Data from Milodowski and Zalasiewicz (1991).⁵ Data from Maynard *et al.* (1986), Appendix.⁶ Data from Garcia-Lopez *et al.* (1997) supplemented with new data by the present author.⁷ Data from Powell (2003).⁸ Data on Archean shales from Watanabe (2002).⁹ Data from van de Kamp and Leake (1997).

X = mineral present, abundance unknown

Table 2. Mean chemical compositions (wt.%) of shales and muds.

Site/formation	Metamorphic grade	#Samples	SiO ₂	TiO ₂	Al ₂ O ₃	Fe ₂ O ₃ ¹⁰	FeO	MnO	MgO	CaO	Na ₂ O	K ₂ O	P ₂ O ₅	Si/Al	Calculated % of silica released from shales during alteration**			
															GOM	California	Amazon	
GOM muds ¹	Pleistocene-modern	50	61.96	0.69	16.56	5.96	0.14	3.75	5.76	2.01	3.12	0.14	3.74					
California muds ²	Pleistocene-modern	40	62.10	0.79	16.21	4.87	1.35	0.12	3.21	5.81	2.63	2.70	0.21	3.83				
Amazon Fan muds ³	Pleistocene-modern	58	62.52	1.05	21.08	7.76	0.11	2.07	0.97	1.46	2.97	0.19	2.97					
Simpson Group shales	Diagenetic zone	18	59.23	0.81	22.41	1.95	3.47	0.09	2.54	0.73	0.83	7.78	0.15	2.64	29.4	31.0	10.8	
Cozy Dell/Matija Fms. ⁴	Late diagenetic zone	6	62.51	0.92	18.44	4.45	3.03	0.07	2.88	1.70	1.78	4.06	0.16	3.39	9.4	11.5	+14.3	
Juncal Fm. ⁴	Late diagenetic zone	6	61.84	0.90	18.37	3.72	4.15	0.09	3.01	2.21	1.91	3.65	0.14	3.37	10.1	12.2	+13.5	
Landovery Shales ⁵	Anchizone	6	61.77	1.19	22.73	7.40	0.09	0.93	0.12	1.17	3.76	0.05	2.72	27.4	29.1	8.4	17.0	
Martinsburg Fm. ⁶	Anchizone	17	58.70	25.90	6.26	1.66	0.36	0.53	6.51	2.27	39.4	40.8				18.1	7.6	+8.4
Applecross Fm. ⁹	Anchizone	5	60.18	1.11	19.37	6.05	1.68	0.11	2.82	0.51	1.38	6.59	0.20	3.11	17.0	18.9	+4.8	14.8
Formigosa Fm.	Anchizone	4	65.16	1.10	22.00	0.10	5.83	0.01	1.10	0.06	0.54	4.00	0.09	2.96	22.7	20.8	0.2	+3.1
Luarca Fm.	Epizone	6	60.38	1.07	23.31	0.33	6.81	0.07	2.03	0.54	0.87	4.41	0.17	2.59	30.8	32.4	12.9	14.1
Keewaywin Fm.	Epizone	4	56.88	1.02	27.55	1.02	2.31	0.06	1.52	1.82	1.44	7.08	0.06	2.06	46.7	46.1	12.7	14.1
Burgess Shale ⁷	Epizone	4	55.13	0.76	25.10	5.20	0.03	2.20	4.36	0.54	6.49	0.16	2.20	41.3	42.7	25.9	30.8	20.1
Kidd Creek, DDH-A ⁸	Epizone	11	66.85	0.81	20.83	4.91	0.05	2.07	0.40	2.09	1.87	0.10	3.21	14.2	16.2	+8.2	8.8	7.9
																	+5.1	

¹ Data from Pickering and Stow (1986), table 1. Hole 616, core sections 1–2 to 16–3 and 28–2 to 34–3 (18 samples); Hole 620, core sections 13–2 to 44–3 (32 samples).

GOM = Gulf of Mexico, samples from offshore Mississippi fan.

² Non-marine muds from drainages of Sierra Nevada and Southern California, unpublished data of author.³ Offshore Amazon Fan, Ocean Drilling Program holes 931, 932, 933, 934, 935, 936, 937, 940, 941, 942. Shipboard Scientific Party (1995)⁴ Data from van de Kamp *et al.* (1976).⁵ Data from Mlodowski and Zalasiewicz (1991).⁶ Data from Maynard *et al.* (1986), Appendix.⁷ Data from Powell (2003).⁸ Data on Archean shales from Watanabe (2002).⁹ Data from van de Kamp and Leake (1997).¹⁰ Where both oxidation states of iron were analyzed, both values are indicated, otherwise total iron, either as FeO or Fe₂O₃ is indicated.

Remainder of samples are authors' data. They include: Ordovician Simpson Group shales at 3.5–5.5 km depths, Anadarko Basin, Oklahoma; Archean Keewaywin Formation shales, Sandy Lake, NW Ontario; Ordovician Luarca Shale, Cabo Penas, Asturias, Spain; Silurian Formigosa Shale, Cabo Penas, Asturias, Spain.

Analyses, minus LOI, H₂O, CO₂ recast to 100%.^{*}Calculated with equation 1 (see text), positive values occur where Si/Al of modern mud is greater than Si/Al of ancient shale.^{**} Values represent SiO₂ in modern muds × proportion of original silica lost (from columns to left).

completely dissolved. The samples were analyzed for major oxides, trace elements, and REE by a combination of inductively coupled plasma (ICP), instrumental neutron activation analysis (INAA), inductively coupled plasma-mass spectrometry, and X-ray fluorescence (XRF) techniques. Calibration was with seven USGS and CANMET reference standards. One of the seven standards was used during the analysis for each group of ten samples. Ferrous Fe, in acid-digested samples, was determined by titration with KMnO₄.

Normative minerals were calculated using the program *SEDNORM*, an extension of the procedure published by Garrels and Mackenzie (1971). The program is available on request from the present author.

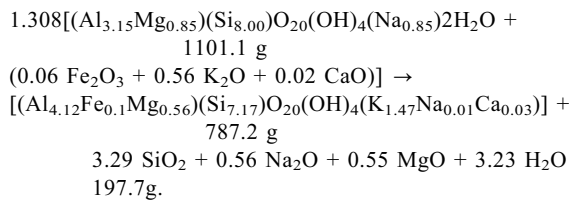
ESTIMATES OF SILICA DERIVED FROM CLAYS AND SHALES

Clay-mineral reactions in the smectite–illite–muscovite series and mud-to-shale-to-schist alterations are considered to demonstrate the decrease in silica content relative to alumina with increasing temperature in burial diagenesis and metamorphism.

Estimates based on balanced equations

Using end-member chemical formulae and molecular weights for smectite, illite, and muscovite, with balanced reactions assuming Al₂O₃ to be constant, estimated silica yields are as follows:

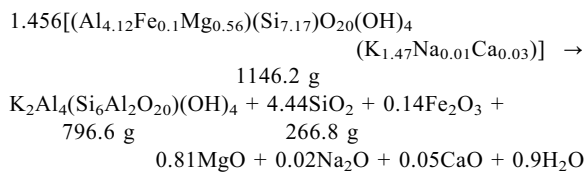
(1) Smectite to illite



Total weight of reaction products = 1101.1 g

Silica released in transformation = $(197.7/1101.1) \times 100 = 18.0\%$

(2) Illite to muscovite



Total weight of reaction products = 1146.2 g

Silica released in transformation = $(266.8/1146.2) \times 100 = 23.3\%$

The sources of the mineral formulae are: smectite, Newman (1987, p. 49); illite, Šrodoň *et al.* (1986, tables 1, 3, #M11); muscovite, Deer *et al.* (1966, p. 201).

The trend of reduced silica relative to alumina for the smectite–illite series, and muscovite, is illustrated in Figure 1a as Si/Al (SiO₂ wt.%/Al₂O₃ wt.%) relative to temperature. The estimated 18% silica loss in the smectite-to-illite transformation occurs in the ~30–190°C range and the further 23.3% silica loss in the illite-to-muscovite transformation occurs in the ~190–500°C range (Figure 1b). Other estimates of silica loss from the smectite to illite reaction, using different mineral compositions (less aluminous smectites) from those used here, yielded 28% SiO₂ (Leder and Park, 1986) and 23.4% SiO₂ (Boles and Franks, 1979). These are also plotted in Figure 1b, as is the calculated silica loss for the illite-to-muscovite transformation of Boles and Franks (1979). These calculations and the temperature-transformation plot (Figure 1b) establish that smectite may lose up to 10% of its original silica content upon reaching 60–70°C during burial and 17–28% in the range 30–200°C. Due to the progressive alteration of smectite to illite in various mixtures of smectite and illite layers, and as illite transforms to muscovite, silica is released throughout the transformation. Thus, over a wide range of increasing burial and temperature, silica is released from clays and is potentially available to migrate from its source, as demonstrated by the general absence of precipitated silica in shales. Concurrent with silica loss is the evolution of water, as smectite is transformed to illite (Figure 1d). Water loss as a proportion of the original 23–24 wt.% in smectite is ~60–70% upon transformation to illite.

The saponite–chlorite transformation, as outlined by equation 2 of Chang *et al.* (1986) with Al conserved, yields 34.5 wt.% SiO₂. For the case of mobile Al (equation 1 of Chang *et al.*, 1986), the silica yield is 6.8 wt.%. These reactions occur at similar temperatures in the diagenetic zone to those of smectite–illite transformation. In shales where both smectite and saponite are present, both will evolve silica upon changing to illite and chlorite, respectively.

Estimates based on Si/Al ratios

An alternative, empirical procedure to evaluate changes in whole-rock Si/Al and silica loss follows. Consider that silica is removed from shales so that the remaining elements are enriched. Assume initially that a shale contains 55 wt.% SiO₂ and 16 wt.% Al₂O₃ with Si/Al = 3.44. Remove 10 wt.% silica so that 49.5 wt.% remains and recalculate the rock analysis to 100% total using the factor $100/94.5 = 1.0582$. This yields SiO₂/Al₂O₃ = $52.38/16.93 = 3.09$. Five successive 10% silica loss increments yield a total loss of 43.7 wt.% of the original silica (Figure 2a). For this plot, I have assumed that for each 100°C increase in temperature, 10% of the silica in shale is lost. A similar procedure was followed to model silica and Na loss as well as K gain for the mean Gulf of Mexico (GOM), California, and Amazon muds (Table 3). The results follow the

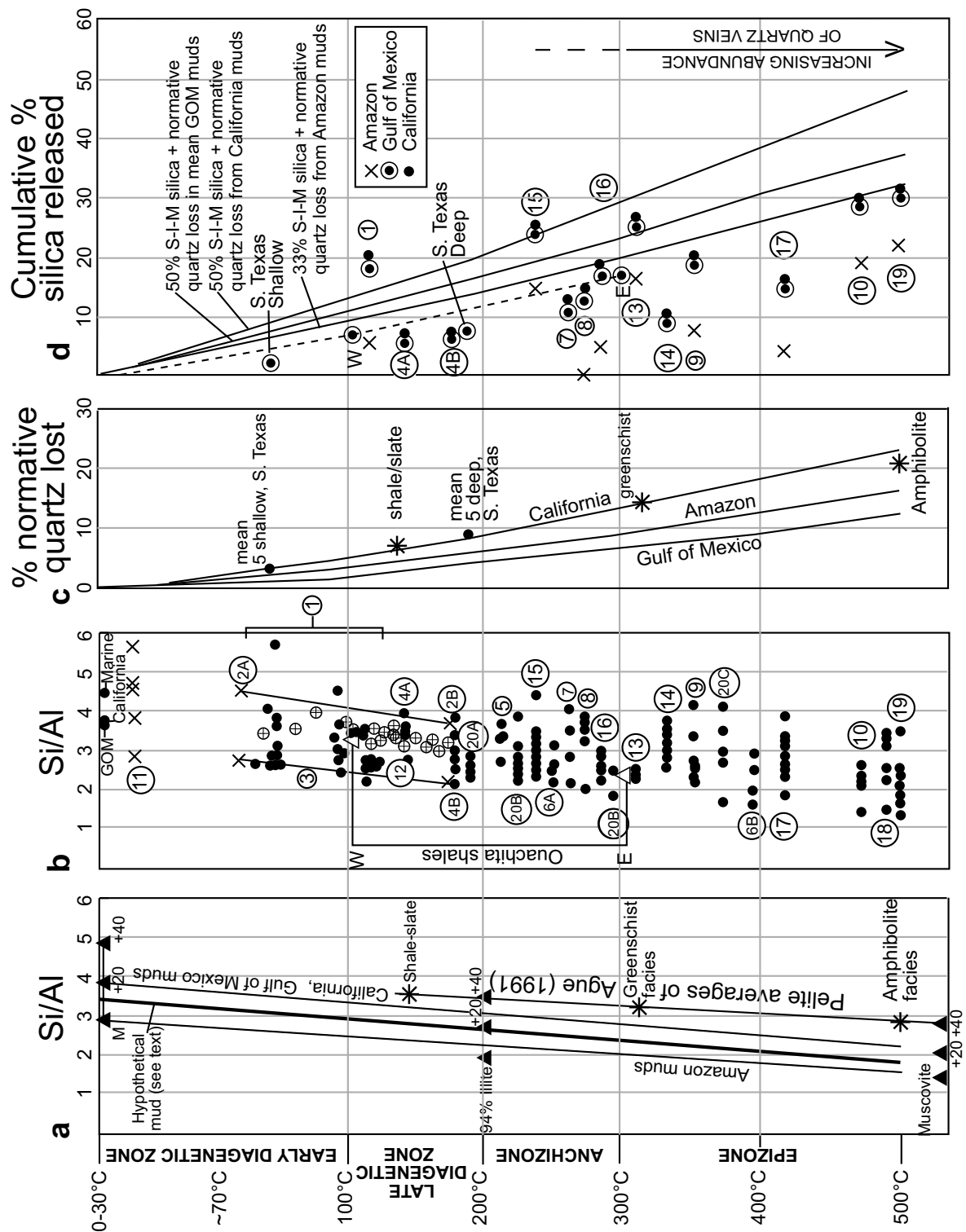


Figure 2. (a) Trends of Si/Al decline in shales with increasing temperature in burial metamorphism. The estimated trend of silica loss of 10% of total silica per 100°C (see text) tracks closely the trend based on means for pelites of various metamorphic grades from Ague (1991). The heavy line represents the assumed mud-shale composition with initial 55% SiO_2 and 16% Al_2O_3 . Also indicated are similar trends for Amazon Fan muds and the overlying California and Gulf of Mexico mud trends. Plots for mixtures of smectite and quartz ($M_e + 20, +40$) where $M_e = \text{smectite}; +20 = \text{smectite plus } 20\% \text{ quartz}; +40 = \text{smectite plus } 40\% \text{ quartz}$, indicate that the most clay-rich shales plot to the left; increasing proportions of quartz shift the data points to the right in Figure 2b. In similar fashion, 94% illite and quartz as well as muscovite and quartz are shown. (b) Si/Al for shales showing the trend of decreasing silica with increasing temperature into the realm of metamorphism (epizone). The trend is similar to the calculated trends in Figure 2a. Modern sediments (Table 1) are plotted at the top of the diagram with various suites of ancient sediments below. The most clay-rich shales plot to the left; increasing proportions of quartz shift the data points to the right. For samples at the left side of the data, normative and modal quartz is 0–10%; toward the right, quartz is in the range 30–50%. The Gulf Coast Tertiary shales (12), plotted as crosses in circles, contain 16–24% quartz (Land *et al.*, 1997). If there were no loss (removal) of silica from the shales, Si/Al would remain similar to starting materials rich in smectite ($\text{Si}/\text{Al} \sim 3–4$). The Ouachita shale data are from Sutton and Land (1997). Numbers refer to: (1) Simpson Group shales*, Ordovician, Anadarko Basin, Oklahoma; (2A) Shale, Cretaceous, Sweetgrass Arch, Montana (Hoffman and Hower, 1979); (2B) shale, Cretaceous, Disturbed Belt, Montana (Hoffman and Hower, 1979); (3) quartz-poor bentonite, Montana (Hoffman and Hower, 1979); (4A) Cozy Dell and Matilija shales (van de Kamp *et al.*, 1976); (4B) Juncal Fm. Shales (van de Kamp *et al.*, 1976); (5) Upper Cretaceous shales*, Santa Ynez Mountains, California; (6A) Jurassic shales, Alps (Frey, 1978, table 5); (6B) Jurassic shales, Alps (Frey, 1978, table 7); (7) Appelcross Fm. shales, Proterozoic (van de Kamp and Leake, 1997); (8) Formigosa Fm. shales*, Silurian, Asturias, Spain (Garcia-Lopez *et al.*, 1997); (9) Luarca Fm. shales*, Ordovician, Spain (Garcia-Lopez *et al.*, 1997); (10) Keewaywin Fm. shales*, Archean, NW Ontario (Corris, 1991); (11) modern marine muds (Maynard *et al.*, 1982); (12) Gulf Coast Tertiary shales (crosses in circles) buried 2.4 to 5.5 km (Land *et al.*, 1997); (13) Burgess Shale (Powell, 2003); (14) Archean shales, Kidd Creek mine, Ontario (Watanabe, 2002); (15) Martinsburg Fm. (Maynard *et al.*, 1982); (16) Llandover shales (Miodowski and Zalasewicz, 1991); (17) Archean shales (Fedo *et al.*, 1996); (18) Grenville schists (Hounslow and Moore, 1967); (19) Dalradian pelites (Atherton, 1968); (20) Devonian and Carboniferous shales, SW Portugal (Abad *et al.*, 2001); (20A) = Mira Fm; (20B) = Brejera Fm; (20C) = Phyllite-Quartzite Fm.; and (20D) = Meriol and Pulo de Lobo Fms. Those marked with * are shales chemically analyzed for this study. (c) Calculated normative quartz abundance losses based on SEDNORM mineralogies for Amazon, Gulf of Mexico (GOM), and California muds (Table 3) in which silica is reduced by 10% for each 100°C increase in burial temperature. These curves are derived by subtracting the amount of normative quartz at successively higher temperatures from the initial value at surface conditions. For comparison, the stars represent normative quartz for mean pelitic values of Ague (1991). (d) Estimated silica losses for shale means relative to various mud compositional means as listed in Table 2. The values were calculated using equation 1 (see text) and then the apparent amount of silica lost from the assumed precursor mud was calculated (Table 2). The curves are for estimated silica losses based on normative quartz lost (from Figure 2c) plus silica released in smectite-illite-muscovite (S-I-M) transformations (Figure 1b). The curve to the left is for feldspar-poor Amazon mud plus 3.3% of silica released from clays; the middle curve is for Gulf of Mexico mud plus 50% of silica from clay; and the curve to the right represents feldspathic California mud plus 50% of silica released from clays. Most shales plot within the area under the curves. The feldspar-poor Simpson and Martinsburg shales associated with quartzose sandstones compare well with Amazon mud but not with the unlikely feldspathic California progenitor. South Texas points are derived from data from Land *et al.* (1997) and represent silica loss relative to the GOM muds mean (Table 2) over the range of burial ($\sim 80–190^\circ\text{C}$) of the shales studied. W indicates the mean of 10 least altered shales and E the mean of 10 most altered shales (Sutton and Land, 1996) for silica loss relative to the GOM mud mean in Table 2. The quartz-vein abundance trend is from Ague (1994b).

trend for clay and mica data (Figure 1a) and the silica loss estimated for shale to amphibolite-facies metapelites by Ague (1991). In the temperature range up to 200°C, as much as 20%+ of the original silica in clay has been released. Up to 40%+ of the original silica in clay has been released from the rock upon reaching 400–500°C. Through the entire temperature range, much of the evolved silica is from smectite-to-illite and illite-to-muscovite transformations, with lesser contributions from feldspar alterations and quartz solution.

Compared to the Si/Al trend in clays (Figure 1a) and the reduction in Si/Al displayed by shales with increasing metamorphism (Figure 2b), the results obtained by this method are reasonable. An advantage of this approach is that it starts with fixed mud compositions, and avoids the uncertainties regarding element mobility introduced by micro- and macro-scale mineral and chemical compositional variations in pelitic rocks, as cited by Moss *et al.* (1996).

Estimates based on shale compositions

Another approach to estimate apparent silica losses is to use mean shale compositions at various levels of diagenesis/metamorphism, compared to modern mud compositions (Tables 1, 2). The modern muds are smectite-rich relative to kaolinite (Table 1) and have mean Si/Al = 3.74 to 4.40. For this comparison, equation 2 of Ague (1991), modified for the specific case of conserved alumina and mobile silica, is used:

$$\begin{aligned} \text{\% silica gain or loss} &= \\ &\left[\left(\frac{\text{Initial alumina}}{\text{Final alumina}} \right) \left(\frac{\text{Final silica}}{\text{Initial silica}} \right) - 1 \right] \times 100 \end{aligned}$$

For various suites of shales compared to modern muds (Table 2), calculated results indicate that 8–47% of original silica was lost during alteration; much of this loss is attributable to clay-mineral transformations.

DISSOLUTION OF DETRITAL QUARTZ IN SHALES

In shales, non-clay detritus includes, by volume <5% to 40% or more, silt-size quartz and feldspar. Evans (1990) estimated that up to 20% of original quartz silt in shales was removed by pressure solution in the anchizone. Also in the anchizone, Sutton and Land (1996) found that significant volumes of quartz were mobilized from shales and deposited in quartz veins. Another example is from diagenetic-zone shales interbedded with sandstones where 20–25% of detrital quartz in the shales was removed by pressure solution (Čyžienė *et al.*, 2006). My own thin-section observations indicate significant quartz dissolution in late diagenetic zone, Simpson Group shales, Oklahoma, and epizone Luarca shales, Spain. In these cases, angular elongate, embayed

quartz grains that are oriented parallel to layering represent remnants of originally larger, more rounded to subangular, equant grains that occur in adjacent silt layers. Similar dissolution of quartz in shales has been observed by Knoke (1966) and Füchtbauer (1978). Apparently, up to half or more of the original detrital quartz silt in the clay-rich beds has been removed in solution. Evidence for pressure solution of quartz in shales altering to slates has been cited by Groshong (1976), Wright and Platt (1982), Evans (1990), and Do Campo and Nieto (2003). In cases of quartz solution in the development of slaty cleavage, studied by Erslev (1998), much of the dissolved silica migrates only short distances (<1 m) and thus is an unlikely source of significant volumes of silica moving over distances of hundreds of meters.

It should be possible to estimate the amount of silica mobilized in burial alteration due to quartz-silt dissolution from decreasing amounts of modal quartz in shales with increasing burial and temperature. Unfortunately, there are no modal mineral abundance data for a single shale from the diagenetic zone into the epizone. Generally, there are few mineral analyses of shales to quantitatively evaluate mineralogical changes with burial metamorphism. A way to address the question of quartz loss with increasing alteration and temperature is to use normative quartz abundances for shales. For this purpose, the California, Gulf of Mexico, and Amazon muds were empirically modeled chemically (Table 3) for silica and Na losses and K gains. The results (Table 3, and Figure 2c) indicate progressively less quartz and greater amounts of phyllosilicates with increasing temperatures of alteration, and they parallel the trends of decreasing silica for shales and clays (Figures 1a, 2b). The normative quartz loss is ~50–70% of the original amount for the cases modeled. The actual amount of normative quartz lost from surface conditions, through the epizone, ranges up to 16–22 wt.%. Within the range of diagenesis, the estimated loss is 6–9 wt.%.

At a given temperature or level of alteration, using the apparent silica losses in the smectite–illite–muscovite transformations (Figure 1b), plus those for quartz dissolution (Figure 2c), the calculated silica losses for shale relative to possible precursor muds can be compared (Figure 2d). For a given case, the total calculated silica loss may exceed the amount of silica derived from clays, but the difference is accounted for by quartz dissolution during diagenesis/metamorphism. For the Miocene-Oligocene shales studied by Land *et al.* (1997), comparing the mean of the five deepest samples to that of the five shallowest samples, normative quartz loss was 5.2%. Land *et al.* (1997) estimated up to 9% silica released in the smectite–illite transformation; half this amount (assuming 50% illite in the shales) plus the 5% quartz loss adds up to 9.5% silica yield from these shales. This is the same as estimated using equation 1, comparing the means of the five shallowest and five

Table 3. Chemical analyses and normative mineralogies.

	Amazon Fan muds						California muds						Gulf of Mexico muds (GOM)					
	1	2	3	4	5	6	1	2	3	4	5	6	1	2	3	4	5	6
SiO ₂	62.52	59.96	57.34	54.75	51.95	49.06	64.69	62.19	59.62	54.34	51.66	66.20	63.74	61.20	58.64	56.00	53.33	
TiO ₂	1.05	1.12	1.19	1.26	1.33	1.40	0.82	0.88	0.94	1.00	1.06	1.12	0.74	0.79	0.84	0.89	0.94	0.99
Al ₂ O ₃	21.08	22.46	23.87	25.32	26.69	28.00	16.88	18.03	19.20	20.39	21.60	22.82	17.69	18.92	20.18	21.43	22.74	24.06
Fe ₂ O ₃	7.19	7.66	8.14	8.64	9.11	9.56	5.07	5.41	5.76	6.12	6.48	6.84	6.37	6.81	7.26	7.73	8.20	8.68
FeO	0.50	0.53	0.56	0.59	0.62	0.65	1.41	1.51	1.61	1.71	1.81	1.91						
MnO	0.11	0.12	0.13	0.14	0.15	0.16	0.12	0.13	0.14	0.15	0.16	0.17	0.15	0.16	0.17	0.18	0.19	0.20
MgO	2.07	2.21	2.35	2.49	2.63	2.76	3.34	3.57	3.80	4.04	4.28	4.52	2.14	2.29	2.44	2.60	2.76	2.92
CaO	0.97	1.03	1.09	1.16	1.23	1.29	1.89	2.02	2.15	2.28	2.41	2.55	1.08	1.17	1.25	1.33	1.41	1.49
Na ₂ O	1.46	1.13	0.78	0.40	0.00	0.00	2.74	2.50	2.24	1.95	1.64	1.31	2.15	1.87	1.56	1.23	0.88	0.51
K ₂ O	2.97	3.70	4.46	5.26	6.07	6.89	2.81	3.53	4.29	5.09	5.92	6.78	3.33	4.10	4.90	5.85	6.74	7.66
P ₂ O ₅	0.19	0.20	0.21	0.22	0.23	0.24	0.22	0.23	0.24	0.25	0.26	0.27	0.15	0.16	0.17	0.18	0.19	0.20
Si/Al	2.97	2.67	2.40	2.16	1.95	1.75	3.83	3.45	3.11	2.80	2.52	2.26	3.74	3.37	3.03	2.74	2.46	2.22
Quartz	31.3	28.3	25.3	22.4	19.6	15.1	30.8	26.4	22.0	17.5	12.9	8.3	36.2	33.0	28.9	24.3	20.0	15.7
Albite	12.3	9.5	6.6	3.4	0.0	0.0	23.2	21.2	19.0	16.5	13.9	11.1	18.1	15.8	13.2	10.4	7.4	4.3
Anorthite	3.6	3.8	4.0	4.3	4.6	4.8	7.9	8.5	9.1	9.7	10.3	10.9	4.4	4.8	5.1	5.4	5.7	6.1
K-feldspar	0.0	0.0	0.0	0.0	0.0	0.0	4.9	8.0	11.4	14.9	18.6	22.4	0.0	1.1	3.9	8.0	11.3	14.8
Fe-chlorite	1.1	1.2	1.2	1.3	1.4	1.5	2.7	2.9	3.1	3.3	3.5	3.7	0.3	0.3	0.3	0.3	0.3	0.4
Mg-chlorite	5.0	5.3	5.6	6.0	6.3	6.6	8.0	8.6	9.1	9.7	10.3	10.9	5.1	5.5	5.9	6.2	6.6	7.0
Muscovite	24.0	29.8	36.0	42.4	49.0	55.6	16.0	17.5	19.1	20.7	22.4	24.1	26.8	31.5	34.2	36.2	38.9	41.6
Kaolinite	14.1	12.8	11.4	9.8	8.2	4.8	0.0	0.0	0.0	0.0	0.0	0.0	1.3	0.0	0.0	0.0	0.0	0.0
Apatite	0.4	0.5	0.5	0.5	0.6	0.5	0.5	0.6	0.5	0.6	0.6	0.6	0.3	0.4	0.4	0.4	0.4	0.5
Hematite	7.2	7.6	8.1	8.6	9.1	9.6	5.1	5.4	5.8	6.1	6.5	6.8	6.3	7.3	7.7	8.2	8.7	
Rutile	1.0	1.1	1.2	1.3	1.3	1.4	0.8	0.9	0.9	1.0	1.1	1.1	0.7	0.8	0.8	0.9	0.9	1.0

For Amazon, California and GOM analyses: #1 is the original mean on a volatile-free basis; #2–6 represent successive iterations of removal of 10% of the SiO₂, 0.4% Na₂O and addition of 0.5% K₂O recalculated to 100%. Each step represents a 100°C increase in temperature. The California and GOM means have been recalculated to 100% after removal of Mg and Ca carbonates.

Estimated % minerals lost in solution:

Quartz	0.0	3.0	6.0	8.9	11.7	16.2	0.0	4.4	8.8	13.3	17.9	22.5	0.0	3.2	7.3	11.9	16.2
Plagioclase	0.0	2.6	5.3	8.2	11.3	11.1	0.0	1.4	3.0	4.9	6.9	9.1	0.0	1.9	4.2	6.7	9.4
																	12.1

deepest shales in the Land *et al.* study (Figure 2d). Approximate temperatures are 80°C (shallow) and 190°C (deep) for these shales.

DISCUSSION

The actual silica available from the smectite–illite–muscovite transformations is up to 50% of original silica in smectite (Figure 1b). However, shales may initially contain 30–50% smectite which, upon conversion to muscovite, would yield at most 15–25% silica in the epizone, less than that indicated by estimates in Table 2 and Figure 2d. If such amounts of silica are mobilized, then additional sources of silica including feldspar dissolution and pressure solution of quartz must contribute. Commonly, shales contain detrital feldspar (Table 1). Alteration of albite to kaolinite plus Na⁺ and silica yields 45.8% SiO₂. Thus, a shale containing 5% albite would yield 2.3% silica, 10% albite would yield 4.6% silica, etc. K-feldspar yields 43% SiO₂ upon alteration to kaolinite, plus K⁺ and silica. In some shales a significant proportion of the feldspar may be dissolved at temperatures of <120°C (Boles and Franks, 1979; Lynch *et al.*, 1997), whereas in others, feldspar is preserved, as in the Keewaywin, Luarca, and Juncal Shales (Table 1). Thus it is difficult to generalize about the contribution of feldspar dissolution to the silica evolved from shales.

Apparently little or none of the mobilized silica remains in shales of the diagenetic zone, as indicated by the general absence of quartz veins or quartz lenses in clay-rich rocks. However, within shales, interlayered laminae of siltstone and fine-grained sandstone commonly contain secondary quartz as overgrowths on detrital grains. A detailed study by Milliken (1994) found authigenic quartz overgrowths on quartz silt grains in some shales but not others. In the same work, no evidence of pressure solution of quartz grains was found. Thus it might be inferred that the authigenic silica was derived from clay transformations. Assuming that silica is expelled from the shales, a likely site for its precipitation is adjacent and updip permeable sandstones in which quartz cement has been added during the same period that clay mineral transformations and silica loss from shales occurred.

If silica is not removed from shales, the overall silica content of the rock should remain constant; volumetrically, the rock will contain more authigenic quartz and less clay with increasing levels of alteration. Chemically, the composition remains the same as before clay transformation, so Si/Al should be constant. In fact, these relations are not observed, indicating that shales act as open systems and much silica and water migrate out of them during alteration, while K is absorbed as illite develops.

The volume of silica imported to sandstone during diagenesis to $T = 130\text{--}150^\circ\text{C}$ and to a depth of

4.2–4.5 km was estimated as 18.9% by Gluyas and Coleman (1992). In the Tuscarora Quartzite, Sibley and Blatt (1976) found that pressure solution accounted for about a third of the 21% quartz cement. For the Norphlet sandstones, Thomas *et al.* (1993) estimated that a minimum of 17–34% of the quartz cement was derived by pressure solution on stylolites. In those cases, an external (to the sandstone) source of quartz cement is necessary, in addition to internal pressure solution of sandstone quartz grains. Stone and Siever (1996) estimated the mean quartz cement added to quartzose sandstones buried to 5 km ($T = 170\text{--}200^\circ\text{C}+$) to be 17.4 vol.% . In their analysis of sources of silica cement, Stone and Siever concluded that 7.6% of the 17.4% came from pressure solution, stylolitization, and various silicate reactions within the sandstone, and the remaining ~10% was imported from outside the sandstones. They suggest the smectite–illite reaction in shales is the external source of silica cement in the sandstones. Assuming 10 vol.% cement in the sandstone, it is possible to estimate the likely availability of silica from adjacent shales. From the estimates outlined above and Figure 1b, ~10% of the silica is produced by the smectite–illite transformation in the 100–200°C range. If it is assumed that mixed-layer smectite–illite is 50% of the shale, then ~5% of silica is produced. In marine basins, downdip, central-basin, shale-rich sediments may be volumetrically significant sources of silica to migrate updip for sandstone cement. Typically, shale is 2–10 times more abundant than sandstone in basins containing quartzose sandstones (Pettijohn, 1975; Statler, 1965; and the present author's own observations). To deposit the required 10% cement in the sandstone, a transfer efficiency of ~20–100% of silica in solution would be necessary.

An estimate of the proportions of silica from the smectite–illite transformation, from dissolution of quartz silt in shale, and from pressure solution of quartz in sandstones interbedded with deep basin shales, using information from the preceding sections, follows. Assume the deep basin rocks are 80% shale and 20% sandstone. For the temperature range 100–200°C, assume 10% silica from the smectite–illite transformation as above. Thus, 80% shale containing 50% clays yields $0.8 \times 0.5 \times 10\% = 4.0\%$ SiO₂. To this, add another 4% SiO₂ for quartz-silt dissolution. From the sandstone, quartz pressure solution yields $0.2 \times 4.0\% = 0.8\%$ SiO₂. The silica total is 8.8%, with 9% of the silica coming from pressure solution of quartz in sandstone, and the rest from shale. The 4% silica by pressure solution comes from an intensely stylolitized sandstone as estimated by Stone and Siever (1996).

Quartz cement is added to sandstones gradually during increasingly deeper and warmer burial, as indicated by layered overgrowths and equilibration temperatures in overgrowths (Marchand *et al.*, 2002). This may mirror the gradual evolution of silica from

clays in shales with increasing burial and temperature. If such gradual and continuous cementation actually occurs, then separate phases or stages of silica precipitation may not be the general case.

OBSERVED SILICA MIGRATION

In the diagenetic zone, common physical evidence of silica migration is quartz overgrowths in sandstones and, in some cases, quartz veins in shales and sandstones. In many cases, fluid inclusions indicate that authigenic quartz was precipitated at temperatures close to ambient formation temperatures (Walderhaug, 1994; Rossi *et al.*, 2002).

Out-of-equilibrium fluid-inclusion temperatures (greater than *in situ* temperatures) in veins, and quartz overgrowths on detrital grains in sandstones, have been documented in numerous studies (Figure 3). These suggest that solution of silica at higher temperatures and greater depths, with subsequent migration to shallower depths and lower-temperature environments. The silica in solution may be from clay-mineral transformations, pressure solution of quartz grains in sandstones, and/or feldspar alterations or some combination of these sources as described above. Movement of fluid from greenschist-facies conditions (270°C) to the diagenetic zone (160°C) was demonstrated by Harrison *et al.* (2004). Aplin and Warren (1994, p. 849) concluded, ‘‘The most ^{18}O -rich waters of the North Sea and Gulf Coast basins, and of quartz-precipitating paleofluids can be explained by the recrystallization of mudstone clay minerals and/or carbonate *in a closed system*’’. In the Gulf Coast, certain waters derived from shales at 60–100°C+, are less saline than sea water and typical Gulf of Mexico Basin formation waters. These waters are supersaturated in silica and have $\delta^{18}\text{O} = +2$ to +9 suggesting they were released in the smectite-to-illite reaction as clay-derived (diagenetic) basinal waters (Szalkowski, 2000; Moran, 2003). Dehydration of clays and other hydrous minerals is responsible for low-salinity waters mixing with saline pore waters in sediments of the Barbados accretionary complex (Gieskes *et al.*, 1990). Such waters, carrying dissolved silica, apparently from the smectite-to-illite transformation, plus possibly, feldspar dissolution, migrate from their deep basin sources to sandstones where quartz cement is precipitated (Girard *et al.*, 2002; Marchand *et al.*, 2002; Rossi *et al.*, 2002; Hogg *et al.*, 1995; Wilkinson *et al.*, 1992). Oxygen isotope ratios in fluid inclusions in quartz cement and veins indicate $T >$ ambient at 3–5 km burial depth in Simpson sandstone in the Anadarko Basin (Figure 2); thus very hot fluids from greater depths migrated into hot sediments at lesser depths (Mitcheltree, 1997). In Frio Fm. sandstones, $\delta^{18}\text{O}$ in quartz cements suggests migration of cementing waters from >1 km deeper in section with possible ‘recycling’ of waters by convection to explain the large

volumes of water required to obtain large volumes of quartz cement (Land *et al.*, 1997). In a detailed quantitative evaluation of the timing and temperature of quartz cement precipitation in Khatatba Fm. sandstones on a structural high, Rossi *et al.* (2002) inferred that hot waters (160°C) were migrated into sandstones at ambient 95 to 130°C. They estimate that sufficient silica-bearing water was supplied from the downdip basin for the observed volume of quartz cement in the sandstones. Typically, sandstones are completely cemented with little remaining porosity in the late diagenetic zone. Evidence of waters warmer than 200°C precipitating quartz in the diagenetic zone is generally unknown; the example of Harrison *et al.* (2004) is an exception.

In the anchizone and epizone, the illite to muscovite transformation is effected with further release of silica. Much of this mobilized silica apparently remains in rocks of these zones as quartz veins in shales and sandstones. Examples include the chlorite and biotite zone metapelites of the Wepawaug Schist (Ague, 1994a,b), anchizone Ouachita shales (Sutton and Land, 1996), Paleozoic metapelites in chlorite and higher zones (Vidale, 1974), Lower Paleozoic anchizone and epizone shales (Richards *et al.*, 2002) in the Cretaceous Kodiak Fm. during anchizone-epizone conditions (Fisher and Brantley, 1992), and in the greenschist-facies Otago Schist (Smith and Yardley, 1999).

CONCLUSIONS

During deep burial of shales, smectites are transformed to illite and, later, to muscovite in the temperature range of 30–500°C. The smectite-to-illite transformation yields 17–28 wt.% SiO_2 as a proportion of the original smectite. The illite-to-muscovite transformation yields a further 17–23 wt.% SiO_2 as a proportion of the original illite. During these alterations, ~60–80% of the water originally contained in smectite is released. The Si/Al in the clays and micas diminishes with increasing alteration as does Si/Al in shales. This indicates a loss of silica from shales rather than retention in shales of silica liberated from clays. The burial metamorphosed rocks are more aluminous and micaceous, and less quartzose than the muds from which they originated.

In this open system, silica loss is ~1% of the gross amount in shale for each 10°C increase in temperature. Thus, for a shale containing 40–50% smectite, ~2.0–2.5 wt.% SiO_2 is evolved over a 50°C temperature range. About 4–9% silica is liberated by dissolution of quartz silt in shales in the realm of diagenesis (to 200°C) and a further 8–15% in the anchizone and epizone (200–500°C). Dissolution and/or kaolinization of feldspars yields 40–45 wt.% silica, so this is a potential source of more silica to migrate from shales, depending on the original detrital feldspar content and the degree of alteration.

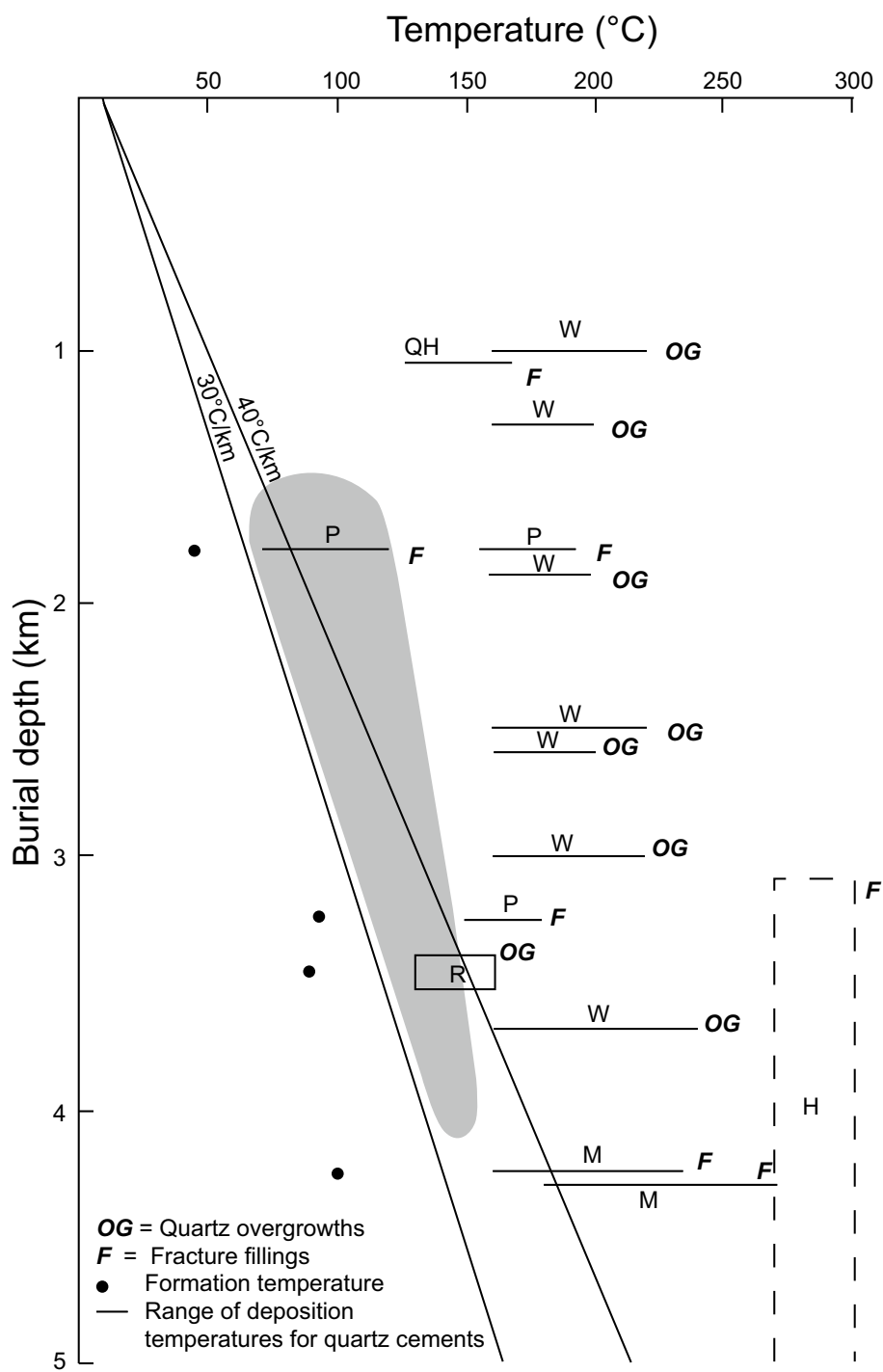


Figure 3. Fluid-inclusion homogenization temperatures for quartz overgrowths on detrital quartz grains and fracture fillings in sandstones plotted against maximum burial temperatures at their sites of deposition. The shaded area is the field of fluid-inclusion homogenization temperatures for quartz cements in many sandstones from Gluyas *et al.* (1993). Many inclusion temperatures are far greater than the ambient formation temperatures suggesting that the secondary quartz was transported in solution from a hotter source. For sedimentary basins, this source is inferred to be basinal shales buried deeper and hotter downdip from the sandstones in which the high-temperature cements were deposited. The apparent movement of silica in solution over vertical distances of 1 km or more implies major mass transfer. Letters above lines representing temperature ranges are for data sources as follows: H = Harrison *et al.* (2004), M = Mitcheltree (1997), P = Parnell *et al.* (2001), QH = Quinn and Haszeldine (2004), R = Rossi *et al.* (2002), W = Wycherly *et al.* (2003).

For the common case in which shale volume exceeds that of sandstone in sedimentary basins, mass balance estimates indicate that ample silica is evolved from clays/shales to provide the silica cement found in sandstones in the diagenetic and late diagenetic zones. In deep or central-basin settings, where shale exceeds sandstone in abundance, the majority of liberated silica is derived from shale. At least some of the free silica has migrated from altering basinal shales (and pressure-solved sandstones) into up-dip sandstones, as proven by quartz overgrowths and fracture fillings (veins), with precipitation temperatures greater than the maximum burial temperatures of the sandstones. Quartz veins are common in anchizone and epizone shales, having been derived from the altering shales themselves.

ACKNOWLEDGMENTS

C. Brime and S. Garcia-Lopez offered guidance for sampling Lower Paleozoic rocks on the Asturian Coast of Spain. R.S. James helped with sampling Archean sedimentary rocks at Sandy Lake in northwest Ontario, and with discussion of the work and review of the manuscript. R.L. Freed and K.P. Helmold provided very careful and insightful manuscript critiques. Eric Eslinger offered helpful comments on the manuscript and Tommie van de Kamp did excellent graphics work. Bob Pendleton offered numerous suggestions to improve grammar. Journal reviewers R.W. Lahann, D.K. McCarty, and A.R. Thomas offered numerous constructive comments to improve the final product.

REFERENCES

- Abad, I., Mata, M.P., Nieto, F., and Velilla, N. (2001) The phyllosilicates in diagenetic-metamorphic rocks of the south Portuguese zone, southwestern Portugal. *The Canadian Mineralogist*, **39**, 1571–1589.
- Ague, J.J. (1991) Evidence for major mass transfer and volume strain during regional metamorphism of pelites. *Geology*, **19**, 855–858.
- Ague, J.J. (1994a) Mass transfer during Barrovian metamorphism of pelites, south-central Connecticut. I: evidence for changes in composition and volume. *American Journal of Science*, **294**, 989–1057.
- Ague, J.J. (1994b) Mass transfer during Barrovian metamorphism of pelites, south-central Connecticut. II: Channelized fluid flow and the growth of staurolite and kyanite. *American Journal of Science*, **294**, 1061–1134.
- Aplin, A.C. and Warren, E.A. (1994) Oxygen isotopic indications of the mechanisms of silica transport and quartz cementation in deeply buried sandstones. *Geology*, **22**, 847–850.
- Atherton, M.P. (1968) The variation in garnet, biotite and chlorite composition in medium grade pelitic rocks from the Dalradian, Scotland, with particular reference to the zonation in garnet. *Contributions to Mineralogy and Petrology*, **18**, 347–371.
- Bjorlykke, K. and Egeberg, P.K. (1993) Quartz cementation in sedimentary basins. *American Association of Petroleum Geologists Bulletin*, **77**, 1538–1548.
- Boles, J.R. and Franks, S.G. (1979) Clay diagenesis in Wilcox sandstones of southwest Texas: implications of smectite diagenesis on sandstone cementation. *Journal of Sedimentary Petrology*, **49**, 55–70.
- Burley, S.D., Mullis, J., and Matter, A. (1989) Timing of diagenesis in the Tartan Reservoir (UK North Sea): constraints from combined cathodoluminescence microscopy and fluid inclusion studies. *Marine and Petroleum Geology*, **6**, 98–120.
- Chang, H.K., Mackenzie, F.T., and Schoonmaker, J. (1986) Comparisons between the diagenesis of dioctahedral and trioctahedral smectite, Brazilian offshore basins. *Clays and Clay Minerals*, **34**, 407–423.
- Cortis, A.L. (1991) Geology, provenance and depositional environment of the Keweenaw Formation, Sandy Lake Greenstone Belt, northwestern Ontario. M.Sc. Thesis, University of Manitoba, Winnipeg, Canada, 265 pp.
- Čžienė, J., Molenaar, N., and Šliaupa, S. (2006) Clay-induced pressure solution as a Si source for quartz cement in sandstones of the Cambrian Deimena Group. *Geologija*, **53**, 8–21.
- Deer, W.A., Howie, R.A., and Zussman, J. (1966) *An Introduction to the Rock-forming Minerals*. Longmans, Green and Co., Ltd., London, 528 pp.
- Do Campo, M. and Nieto, F. (2003) Transmission electron microscopy study of very low-grade metamorphic evolution in Neoproterozoic pelites of the Puncoviscana formation (Cordillera Oriental, NW Argentina). *Clay Minerals*, **38**, 459–481.
- Erslev, E.A. (1998) Limited, localized nonvolatile element flux and volume change in Appalachian slates. *Geological Society of America Bulletin*, **110**, 900–915.
- Eslinger, E., Highsmith, P., Albers, D., and De Mayo, B. (1979) Role of iron reduction in the conversion of smectite to illite in bentonites in the Disturbed Belt, Montana. *Clays and Clay Minerals*, **27**, 327–338.
- Evans, I.J. (1990) Quartz dissolution during shale diagenesis, implications for quartz cementation in sandstones. *Chemical Geology*, **89**, 239–240.
- Fedo, C.M., Eriksson, K.A., and Krogstad, E.J. (1996) Geochemistry of shales from the Archean (~3.0 Ga) Buhwa Greenstone Belt, Zimbabwe: implications for provenance and source-area weathering. *Geochimica et Cosmochimica Acta*, **60**, 1751–1763.
- Fisher, D.M. and Brantley, S.L. (1992) Models of quartz overgrowth and vein formation: Deformation and episodic fluid flow in an ancient subduction zone. *Journal of Geophysical Research*, **97**, 20043–20061.
- Fleet, M.E. and Howie, R.A. (2003) *Rock-Forming Minerals, 3A, Sheet Silicates: Micas*, 2nd edition. Geological Society, London, 756 pp.
- Frey, M. (1978) Progressive low-grade metamorphism of a Black Shale Formation, Central Swiss Alps, with special reference to pyrophyllite and margarite bearing assemblages. *Journal of Petrology*, **19**, 95–135.
- Füchtbauer, H. (1978) Zer herkunft des Quarzzelements, abschätzung der Quarzauflösung in silt- und sandsteinen. *Contributions to Mineralogy and Petrology*, **67**, 991–1008.
- Garcia-Lopez, S., Brime, C., Bastida, F., and Sarmiento, G.N. (1997) Simultaneous use of thermal indicators to analyse the transition from diagenesis to metamorphism: an example from the Variscan Belt of northwest Spain. *Geological Magazine*, **134**, 323–334.
- Garrels, R.M. and Mackenzie, F.T. (1971) *Evolution of Sedimentary Rocks*. W.W. Norton & Company, New York, 397 pp.
- Gieskes, J.M., Vrolijk, P., and Blanc, G. (1990) Hydrogeochemistry of the northern Barbados accretionary complex transect. *Journal of Geophysical Research*, **95**, 8809–8818.
- Giles, M.R., Indrelid, S.L., Beynon, G., and Amthor, J. (2000) The origin of large-scale quartz cementation: evidence from large data sets and coupled heat-fluid mass transport modelling. Pp. 21–38 in: *Quartz Cementation in*

- Sandstones* (R.H. Worden and S. Morad, editors). Special Publication **29**, International Association of Sedimentologists, Blackwells, Oxford, UK.
- Girard, J.P., Munz, I.A., Johansen, H., Lacharpagne, J.-C., and Sommer, F. (2002) Diagenesis of the Hild Brent sandstones, northern North Sea: isotopic evidence for the prevailing influence of deep basinal water. *Journal of Sedimentary Research*, **72**, 746–759.
- Guyas, J. and Coleman, M. (1992) Material flux and porosity changes during sediment diagenesis. *Nature*, **356**, 52–54.
- Guyas, J., Robinson, A.G., Emery, D., Grant, S.M., and Oxtoby, N.H. (1993) The link between petroleum emplacement and sandstone cementation. Pp. 1395–1402 in: *Petroleum Geology of Northwest Europe: Proceedings of the 4th Conference* (J.R. Parker, editor). Geological Society, London.
- Guyas, J., Garland, C., Oxtoby, N.H., and Hogg, A.J.C. (2000) Quartz cement: the Miller's Tale. Pp. 199–218 in: *Quartz Cementation in Sandstones* (R.H. Worden and S. Morad, editors). Special Publication **29**, International Association of Sedimentologists, Blackwells, Oxford, UK.
- Gold, P.B. (1987) Textures and geochemistry of authigenic albite from Miocene sandstone, Louisiana Gulf Coast. *Journal of Sedimentary Petrology*, **57**, 353–362.
- Grim, R.E. (1968) *Clay Mineralogy*, 2nd edition. McGraw-Hill, New York, 596 pp.
- Groshong, R.H. (1976) Strain and pressure solution in the Martinsburg Slate, Delaware Water Gap, New Jersey. *American Journal of Science*, **276**, 1131–1146.
- Harrison, M.J., Marshak, S., and Onasch, C.M. (2004) Stratigraphic control of hot fluids on anthracitization, Lackawanna synclinorium, Pennsylvania. *Tectonophysics*, **378**, 85–103.
- Hartmann, B.H., Juhász-Bodnár, K., Ramseyer, K., and Matter, A. (2000) Polyphased quartz cementation and its sources: a case study from the Upper Paleozoic Haushi Group sandstones, Sultanate of Oman. Pp. 253–270 in: *Quartz Cementation in Sandstones* (R.H. Worden and S. Morad, editors). Special Publication **29**, International Association of Sedimentologists, Blackwells, Oxford, UK.
- Hoffman, J. and Hower, J. (1979) Clay mineral assemblages as low grade metamorphic geothermometers: application to the thrust faulted Disturbed Belt of Montana, U.S.A. Pp. 55–79 in: *Aspects of Diagenesis* (P.A. Scholle and P.R. Schlüger, editors). Special Publication, **26**, Society of Economic Paleontologists and Mineralogists.
- Hogg, A.J.C., Pearson, M., Fallackson, A.E., and Hamilton, P.J. (1995) An integrated thermal and isotopic study of the diagenesis of the Brent Group, Alwyn South, U.K. North Sea. *Applied Geochemistry*, **10**, 531–546.
- Hounslow, A.W. and Moore, J.M. (1967) Chemical petrology of Grenville schists near Fernleigh, Ontario. *Journal of Petrology*, **8**, 1–28.
- Hower, J. and Mowatt, T.C. (1966) The mineralogy of illites and mixed-layer illite/montmorillonites. *American Mineralogist*, **51**, 825–854.
- Hower, J., Eslinger, E., Hower, M.E., and Perry, E.A. (1976) Mechanism of burial metamorphism of argillaceous sediment: 1. Mineralogical and chemical evidence. *Geological Society of America Bulletin*, **87**, 725–737.
- Hunziker, J.C., Frey, M., Clauer, N., Dallmeyer, R.D., Friedrichsen, H., Flehmig, W., Hochstrasser, K., Roggwiler, P., and Schwander, H. (1986) The evolution of illite to muscovite: mineralogical and isotopic data from the Glarus Alps, Switzerland. *Contributions to Mineralogy and Petrology*, **92**, 157–180.
- Inoue, A., Lanson, B., Marques-Fernandez, M., Sakharov, B.A., Murakami, T., Meunier, A., and Beaufort, D. (2005) Illite-smectite mixed-layer minerals in the hydrothermal alteration of volcanic rocks: 1. One-dimensional XRD structure analysis and characterization of component layers. *Clays and Clay Minerals*, **53**, 423–439.
- Knoke, R. (1966) Untersuchungen zur diagenese an kalkkonkretionen und umgebenden tonschiefern. *Contributions to Mineralogy and Petrology*, **12**, 139–167.
- Land, L.S. and Milliken, K.L. (2000) Regional loss of SiO₂ and CaCO₃, and gain of K₂O during burial diagenesis of Gulf Coast mudrocks, USA. Pp. 183–197 in: *Quartz Cementation in Sandstones* (R.H. Worden and S. Morad, editors). Special Publication **29**, International Association of Sedimentologists, Blackwells, Oxford, UK.
- Land, L.S., Mack, L.E., Milliken, K.E., and Lynch, F.L. (1997) Burial diagenesis of argillaceous sediment, south Texas Gulf of Mexico sedimentary basin: A reexamination. *Geological Society of America Bulletin*, **109**, 2–15.
- Leder, F. and Park, W.C. (1986) Porosity reduction in sandstone by quartz overgrowth. *American Association of Petroleum Geologists Bulletin*, **70**, 1713–1728.
- Li, G., Peacor, D.R., Merriman, R.J., and Roberts, B. (1994) The diagenetic to low-grade metamorphic evolution of matrix white micas in the system muscovite-paragonite in a mudrock from central Wales, United Kingdom. *Clays and Clay Minerals*, **42**, 369–381.
- Livi, K.J.T., Veblen, D.R., Ferry, J.M., and Frey, M. (1997) Evolution of 2:1 layered silicates in low-grade metamorphosed Liassic shales of Central Switzerland. *Journal of Metamorphic Geology*, **15**, 323–344.
- Lynch, F.L. (1997) Frio shale mineralogy and the stoichiometry of the smectite-to-illite reaction: the most important reaction in clastic sedimentary diagenesis. *Clays and Clay Minerals*, **45**, 618–631.
- Lynch, F.L., Mack, L.E., and Land, L.S. (1997) Burial diagenesis of illite/smectite in shales and the origins of authigenic quartz and secondary porosity in sandstones. *Geochimica et Cosmochimica Acta*, **61**, 1995–2006.
- Marchand, A.M.E., Macaulay, C.I., Haszeldine, R.S., and Fallackson, A.E. (2002) Pore water evolution in oilfield sandstones: constraints from oxygen isotope microanalyses of quartz cement. *Chemical Geology*, **191**, 285–304.
- Maynard, J.B., Valloni, R., and Yu, H.-S. (1982) Composition of modern deep-sea sands from arc-related basins. Pp. 551–561 in: *Trench-forearc Geology: Sedimentation and Tectonics on Modern and Ancient Active Plate Margins* (J.K. Leggett, editor). Special Publication no. **10**, Geological Society of London.
- Merriman, R.J. and Frey, M. (1999) Patterns of very low-grade metamorphism in metapelitic rocks. Chapter 3 in: *Low-Grade Metamorphism* (M. Frey and D. Robinson, editors). Blackwell Science Ltd., Oxford, UK, 313 pp.
- Merriman, R.J. and Peacor, D.R. (1999) Very low-grade metapelites: mineralogy, microfabrics and measuring reaction progress. Chapter 2 in: *Low-Grade Metamorphism* (M. Frey and D. Robinson, editors). Blackwell Science Ltd., Oxford, UK, 313 pp.
- Milliken, K.L. (1994) Cathodoluminescent textures and the origin of quartz silt in Oligocene mudrocks, south Texas. *Journal of Sedimentary Research*, **A64**, 567–571.
- Milodowski, A.E. and Zalasiewicz, J.A. (1991) Redistribution of rare earth elements during diagenesis of turbidite/hemipelagic mudrock sequences of Llandovery age from central Wales. Pp. 101–124 in: *Developments in Sedimentary Provenance Studies* (A.C. Morton, S.P. Todd, and P.D.W. Haughton, editors). Special Publication no. **57**, Geological Society of London.
- Mitcheltree, D.B. (1997) Basin and thermal history, geochemistry and pressure development of the Simpson Group (Middle Ordovician) based on part of Garvin, Grady and McClain Counties, the Anadarko Basin, Oklahoma. PhD thesis, University of Tulsa, 294 pp.

- Moran, K. (2003) Compositional systematics of deep, low salinity waters in the Upper Wilcox of southeastern Texas. MSc thesis, Louisiana State University, 142 pp.
- Moss, B.E., Haskin, L.A., and Dymek, R.F. (1996) Compositional variations in metamorphosed sediments of the Littleton Formation, New Hampshire, and the Carrabassett Formation, Maine, at sub-hand specimen, outcrop, and regional scales. *American Journal of Science*, **296**, 473–505.
- Newman, A.C.D. (1987) *Chemistry of Clays and Clay Minerals*. Monograph **6**, Mineralogical Society, London, 480 pp.
- Parnell, J., Middleton, D., Honghan, C., and Hall, D. (2001) The use of integrated fluid inclusion studies in constraining oil charge history and reservoir compartmentation: examples from the Jeanne d'Arc Basin, offshore Newfoundland. *Marine and Petroleum Geology*, **18**, 535–549.
- Pettijohn, F.J. (1975) *Sedimentary Rocks, 3rd edition*. Harper & Row, New York.
- Pickering, K.T. and Stow, D.A. (1986) Inorganic major, minor, and trace element geochemistry and clay mineralogy of sediments from the deep sea drilling project leg 96, Gulf of Mexico. *Initial Reports of the Deep Sea Drilling Project* (A.H. Bouma, J.M. Coleman, A.W. Meyer *et al.*, editors), **96**, 733–745.
- Powell, W. (2003) Greenschist-facies metamorphism of the Burgess Shale and its implications for models of fossil formation and preservation. *Canadian Journal of Earth Sciences*, **40**, 13–25.
- Quinn, O.F. and Haszeldine, R.S. (2004) Quartz cementation of a faulted sandstone at shallow burial: petrographic and poroperm data: UK North Sea. *Search and Discovery article #90027*, <http://www.searchanddiscovery.net/documents/abstracts/hedberg2004austin/index.htm>
- Richards, I.J., Connelly, J.B., Gregory, R.T., and Gray, D.R. (2002) The importance of diffusion, advection, and host-rock lithology on vein formation: A stable isotope study from the Paleozoic Ouachita orogenic belt, Arkansas and Oklahoma. *Geological Society of America Bulletin*, **114**, 1343–1355.
- Rossi, C., Goldstein, R.H., Ceriani, A., and Marfil, R. (2002) Fluid inclusions record thermal and fluid evolution in reservoir sandstones, Khatatba Formation, Western Desert, Egypt: A case for fluid injection. *American Association of Petroleum Geologists Bulletin*, **86**, 1775–1799.
- Shipboard Scientific Party (1995) Sites 931–942 (R.D. Flood, D.J.W. Piper, A. Klaus *et al.*, editors). *Proceedings of the Ocean Drilling Program, Initial Reports*, **155**, 123–567.
- Sibley, D.F. and Blatt, H. (1976) Intergranular pressure solution and cementation of the Tuscarora Quartzite. *Journal of Sedimentary Petrology*, **46**, 881–896.
- Smith, M.P. and Yardley, B.W.D. (1999) Fluid evolution during metamorphism of the Otago Schist, New Zealand: (1) evidence from fluid inclusions. *Journal of Metamorphic Geology*, **17**, 173–186.
- Spötl, C., Houseknecht, D.W., and Riciputi, L.R. (2000) High-temperature quartz cement and the role of stylolites in a deep gas reservoir, Spiro Sandstone, Arkoma Basin, USA. Pp. 281–297 in: *Quartz Cementation in Sandstones* (R.H. Worden and S. Morad, editors). Special Publication **29**, International Association of Sedimentologists, Blackwells, Oxford, UK.
- Środoń, J., Morgan, D.J., Eslinger, E.V., Eberl, D.D., and Karlinger, M.R. (1986) Chemistry of illite-smectite and end-member illite. *Clays and Clay Minerals*, **34**, 368–378.
- Statler, A.T. (1965) Stratigraphy of the Simpson Group in Oklahoma. *Tulsa Geological Society Digest*, **33**, 162–209.
- Stone, W.N. and Siever, R. (1996) Quantifying compaction, pressure solution and quartz cementation in moderately- and deeply-buried quartzose sandstones from the greater Green River Basin, Wyoming. Pp. 129–150 in: *Siliciclastic Diagenesis and Fluid Flow: Concepts and Applications* (L.J. Crossey, R. Loucks, and M.W. Totten, editors). SEPM Special Publication No. **55**, Society for Sedimentary Geology, Tulsa, Oklahoma.
- Sutton, S.J. and Land, L.S. (1996) Postdepositional chemical alteration of Ouachita shales. *Geological Society of America Bulletin*, **108**, 978–991.
- Szalkowski, D.S. (2000) Low salinity waters in deep sedimentary basins. M.Sc. thesis, Louisiana State University, 231 pp.
- Thomas, A.R., Dahl, W.R., Hall, C.M., and York, D. (1993) $^{40}\text{Ar}/^{39}\text{Ar}$ analyses of authigenic muscovite, timing of stylolitization, and implications for pressure solution mechanisms; Jurassic Norphlet Formation, offshore Alabama. *Clays and Clay Minerals*, **41**, 269–279.
- Thomson, A. (1959) Pressure solution and porosity. Pp. 92–111 in: *Silica in Sediments* (H.A. Ireland, editor). SEPM Special Publication **7**, Society of Sedimentary Geology, Tulsa, Oklahoma.
- Towe, K.M. (1962) Clay mineral diagenesis as a possible source of silica cement in sedimentary rocks. *Journal of Sedimentary Petrology*, **32**, 26–28.
- Van de Kamp, P.C., Leake, B.E., and Senior, A. (1976) The petrography and geochemistry of some Californian arkoses with application to identifying gneisses of metasedimentary origin. *Journal of Geology*, **84**, 195–212.
- Van de Kamp, P.C. and Leake, B.E. (1997) Mineralogy, geochemistry, provenance and sodium metasomatism of Torridonian rift basin clastic rocks, NW Scotland. *Scottish Journal of Geology*, **33**, 105–124.
- Vidale, R.J. (1974) Vein assemblages and metamorphism in Dutchess County, New York. *Geological Society of America Bulletin*, **85**, 303–306.
- Walderhaug, O. (1994) Temperatures of quartz cementation in Jurassic sandstones from the Norwegian continental shelf—evidence from fluid inclusions. *Journal of Sedimentary Research*, **64**, 311–323.
- Walderhaug, O. and Bjorkum, P.A. (2003) The effect of stylolite spacing on quartz cementation in the Lower Jurassic Stø Formation, southern Barents Sea. *Journal of Sedimentary Research*, **73**, 146–156.
- Watanabe, Y. (2002) The late Archean biosphere: Implications of organic and inorganic geochemistry of marine shales and terrestrial paleosols. PhD thesis, Pennsylvania State University, 169 pp.
- Wilkinson, M., Crowley, S.F., and Marshall, J.D. (1992) Model for evolution of oxygen isotope ratios in the pore fluids of mudrocks during burial. *Marine and Petroleum Geology*, **9**, 98–105.
- Wilkinson, M., Milliken, K.L., and Haszeldine, S. (2001) Systematic destruction of K-feldspar in deeply buried rift and passive margin sandstones. *Journal of the Geological Society, London*, **158**, 675–683.
- Wintsch, R.P. and Kvare, C.M. (1994) Differential mobility of elements in burial diagenesis of siliciclastic rocks. *Journal of Sedimentary Research*, **64**, 349–361.
- Wright, T.O. and Platt, L.B. (1982) Pressure dissolution and cleavage in the Martinsburg Slate. *American Journal of Science*, **282**, 122–135.
- Wycherley, H.L., Parnell, J., Watt, G.R., Chen, H., and Boyce, A.J. (2003) Indicators of hot fluid migration in sedimentary basins: evidence from the UK Atlantic Margin. *Petroleum Geoscience*, **9**, 357–374.

(Received 1 August 2006; revised 23 August 2007;
Ms. 1201; A.E. Douglas K. McCarty)